

UCSF

UC San Francisco Previously Published Works

Title

Monitoring lesion activity on primary teeth with CP-OCT and SWIR reflectance imaging

Permalink

<https://escholarship.org/uc/item/24z290zt>

Journal

Lasers in Surgery and Medicine, 55(6)

ISSN

0196-8092

Authors

Zhu, Yihua

Kim, Jungsoo

Lin, Brent

et al.

Publication Date

2023-08-01


DOI

10.1002/lsm.23677

Peer reviewed

BASIC SCIENCE ARTICLE

Monitoring lesion activity on primary teeth with CP-OCT and SWIR reflectance imaging

Yihua Zhu MS | Jungsoo Kim DDS, MS | Brent Lin DMD | Daniel Fried MS, PhD 

School of Dentistry, University of California
San Francisco, San Francisco, California, USA

Correspondence

Daniel Fried, MS, PhD, School of Dentistry,
University of California San Francisco, 707
Parnassus Ave, CA 94143-0758, USA.
Email: daniel.fried@ucsf.edu

Abstract

Objective: The purpose of this study was to use cross polarization optical coherence tomography (CP-OCT) and short wavelength infrared imaging (SWIR) reflectance imaging to monitor changes in the structure and activity of early occlusal caries on primary teeth over a period of 6 months during intervention with fluoride.

Methods: Participants ($n = 29$) aged 6–10 each with two suspected active occlusal lesions on primary teeth completed the study. Fluoride varnish was applied to tooth surfaces every 3-months and participants were instructed to brush twice daily with a fluoride toothpaste. Images were acquired using CP-OCT every 3 months for 6 months. SWIR reflectance images were acquired during forced air-drying of the lesions for 30 s at 0 and 6-months.

Results: Most of the 42 lesions appeared initially active at baseline. Only 6 lesions appeared arrested at baseline based on the presence of a highly mineralized transparent surface layer (TSL) in CP-OCT images. At 6 months, 14 of the lesions appeared arrested including the 6 initially arrested lesions and the TSL thickness increased significantly ($p < 0.0001$). The mean lesion depth (Ld) and the integrated reflectivity over the lesion depth (ΔR) increased significantly ($p < 0.05$) after 6 months for the 42 lesions analyzed. SWIR reflectance images showed that there was a significantly higher ($p < 0.05$) delay before changes in intensity were measured for active lesions versus arrested lesions during lesion drying.

Conclusion: CP-OCT was able to monitor changes in lesion structure and activity including the formation of a highly mineralized TSL indicative of lesion arrest during nonsurgical intervention. Time-resolved SWIR reflectance imaging also shows that there are differences in the dehydration kinetics between active and arrested lesions. This study demonstrates two independent imaging methods that can be used to monitor changes in lesion activity over time.

KEYWORDS

caries detection, caries diagnosis, dental caries, lesion activity, optical coherence tomography, SWIR imaging

INTRODUCTION

The accurate assessment of lesion activity is essential for the effective clinical management of caries lesions. Caries lesions are arrested by the preferential deposition of mineral at the lesion surface that forms an outer layer of higher mineral content that serves as a barrier to the

further diffusion of fluids into the body of the porous lesion.^{1–3} The highly mineralized outer surface zone or transparent surface layer (TSL) can be detected using transverse microradiography and polarized light microscopy that require destruction of the tooth, or in the case of microcomputed tomography cannot be used in vivo. Early occlusal caries is diagnosed by visual-tactile

Yihua Zhu and Jungsoo Kim shared first authorship.

methods. Radiographs are not effective for early caries lesions that have not penetrated deep into the underlying dentin due to the overlapping topography of the crown. For pit and fissure caries, the tactile method via probing with an explorer showed low sensitivity and has been found to be unreliable in its diagnosis.⁴ The occlusal pits and fissures are often heavily stained obscuring early demineralization, often leading to false positives via visual diagnosis.^{5–7}

New non-destructive diagnostic tools are needed that can assess lesion activity in a single visit and monitor changes in the activity of the lesions over time during nonsurgical intervention. Several studies have shown that short wavelength infrared (SWIR) imaging methods such as optical coherence tomography (OCT) at 1310 nm and time-resolved reflectance imaging at wavelengths greater than 1400 nm can be used to assess remineralization and lesion activity.^{8–12} The purpose of this study is to test the hypothesis that both of these SWIR imaging methods can detect changes in lesion activity over time *in vivo*.

When lesions become arrested by mineral deposition in the outer layers of the lesion forming a highly mineralized surface zone, the diffusion of fluids into the lesion is inhibited. Therefore, the rate of water loss and the evaporation dynamics can be related to changes in lesion structure and porosity. Changes in fluorescence loss,^{13–15} thermal emission, and SWIR reflectance^{10,11,16–20} have been investigated as methods for assessing lesion severity and activity. Normal enamel is transparent at SWIR wavelengths, whereas early demineralization causes increased SWIR reflectance due to scattering.²¹ Water in the pores at the surface of the lesion absorbs the incident SWIR light, particularly at wavelengths greater than 1400 nm, reducing surface scattering and lesion contrast.^{22,23} Loss of that water due to evaporation produces a marked increase in reflectivity and lesion contrast. *In vivo* studies have been reported utilizing the fluorescence loss of white spot lesions on coronal surfaces¹⁵ and thermal imaging to assess root caries during dehydration.²⁴ This study is the first clinical study to employ SWIR reflectance imaging during lesion dehydration to assess lesion activity.

OCT can provide high resolution cross-sectional images of lesion structure noninvasively.^{25,26} Polarization-sensitive OCT (PS-OCT) and cross polarization OCT (CP-OCT) utilize the polarization properties of back-reflected light to obtain additional contrast in OCT images and reduce the interference of the strong reflections that occur at tooth surfaces.^{27–30} *In vivo* studies using CP-OCT were able to accurately detect both early and severe occlusal lesions that were not visible on radiographs.^{31,32}

Several studies have demonstrated that CP-OCT is able to monitor remineralization on tooth surfaces by detecting the formation of the highly mineralized TSL on the lesion surface and a decrease in the integrated reflectivity over the lesion depth (ΔR) after exposure to

a remineralization solution.^{8,9,33} *In vitro* studies have shown that the presence of even a thin TSL of less than 20 μm in CP-OCT images reduces lesion activity significantly.³⁴ Removing the TSL on the lesions of extracted teeth in turn produces a corresponding rise in the permeability providing further confirmation of the role of the TSL in arresting lesions.³⁵ Methods have been developed to automatically measure the thickness of the TSL and ΔR from CP-OCT images.^{36,37} In a previous *in vivo* study, CP-OCT was used to monitor changes in the activity of smooth surface enamel lesions on permanent teeth.¹² Even though the test subjects recruited were required to have active lesions based on conventional visual/tactile assessment, CP-OCT imaging indicated that most of the lesions (62/63) had TSLs at baseline suggesting they were already arrested. CP-OCT images indicated there was no significant increase in lesion severity (ΔR) for those lesions measured after 30 weeks providing further confirmation they were indeed arrested. Primary teeth were chosen for this study to ensure that a higher percentage of the lesions would be initially active rather than arrested to demonstrate that changes in lesion severity and activity can be successfully monitored. In addition, lesions progress more rapidly in primary teeth than in permanent teeth due to the thinner layer of enamel requiring more frequent monitoring.

MATERIALS AND METHODS

Participant recruitment and procedures

Study participants ($n = 30$ with 60 primary molars) aged 6–10 were recruited from the UCSF Pediatric Dentistry clinic by the study investigators (UCSF IRB 18-25927). One participant was lost to follow-up after the first visit and was excluded from the study. A total of 29 participants ($n = 29$ with 58 primary molars) completed the study. Participants were required to have at least two primary teeth with suspected pit and fissure caries. Lesions with obvious cavitation, existing restorations covering the pits and fissures or severe enough to require restorative treatment were rejected.

All 58 lesions were visually scored as a 1 in severity according to the International Caries Detection and Assessment System (ICDAS).³⁸ CP-OCT and SWIR imaging showed that 6 of the lesions were likely false positives since no demineralization was observed in the images at any of the three time-points. Color images of each tooth were acquired at the initial visit and at month-6 using a FocusDent MD740 1280 \times 960-pixel intraoral camera. Fluoride varnish was applied to all lesions at 3-month intervals over a period of 6-months to promote remineralization. In addition, the participants were given a fluoride toothpaste with 0.76% monofluorophosphate and instructed to brush twice a day.

Time-resolved SWIR reflectance imaging at 1400–1750 nm

An image of the fully assembled SWIR reflectance imaging device is shown in Figure 1A along with diagrams of the 3D printed probe and its components. The reflectance probe was designed in Fusion 360 from Autodesk and 3D printed using a Form 3 printer from Formlabs. The reflectance probe body consists of a right-angle aluminum mirror to collect light from the occlusal surface and an attachment for the reflectance fiber.³⁹ A low-OH optical fiber of 1 mm diameter fiber is inserted into a cylindrical Teflon plug (3.2×40 mm). Light exiting the plug is directed toward the tooth occlusal surface. There is an air nozzle attached to the reflectance body near the mirror to prevent fogging of the mirror and dehydrate the lesion surface to assess lesion activity.^{10,11,20} The SWIR reflectance images were captured using a 640×480 -pixel micro-SWIR camera (SU640CSX) measuring only $32 \times 32 \times 28$ mm from Sensors Unlimited. Two planoconvex antireflection coated lenses of 60 and 100 mm focal length along with an adjustable aperture were placed between the hand-piece and the InGaAs camera to provide a field of view of 11 mm^2 at the focus plane. SWIR light from a compact tungsten halogen lamp Model SLS201 from Thorlabs with a 1400 nm long-pass filter illuminated the occlusal surfaces.

Images were recorded at 4 Hz for the 30 s time window at 0 and 6-months and imported into MATLAB for further analysis. Profiles of intensity versus time were extracted from the mean intensity of a 5×5 -pixel region of interest that was manually selected. Lesions were designated as active or arrested based on the presence of a transparent surface zone (TSL) from the corresponding CP-OCT images. Unpaired *t*-tests were used to compare SWIR data between suspected arrested and active lesions.

CP-OCT

The CP-OCT system used for this study was the Model IVS-3000-CP purchased from Santec. It operates at a wavelength of 1321 nm with a bandwidth of 111 nm ($11.4 \mu\text{m}$ axial-resolution) and it is capable of acquiring complete tomographic images $6 \times 6 \times 7$ mm in approximately 3 s. Images of the CP-OCT handpiece are shown in Figure 1B. It has been used for multiple in vivo caries imaging studies.^{12,30,32}

An appliance made of autoclavable Dental SG resin printed using a 3D printer, Formlabs 2 was placed on the distal end of the OCT scanning handpiece and the handpiece was covered with polyethylene film for infection control. Air at 10 psi was connected to the

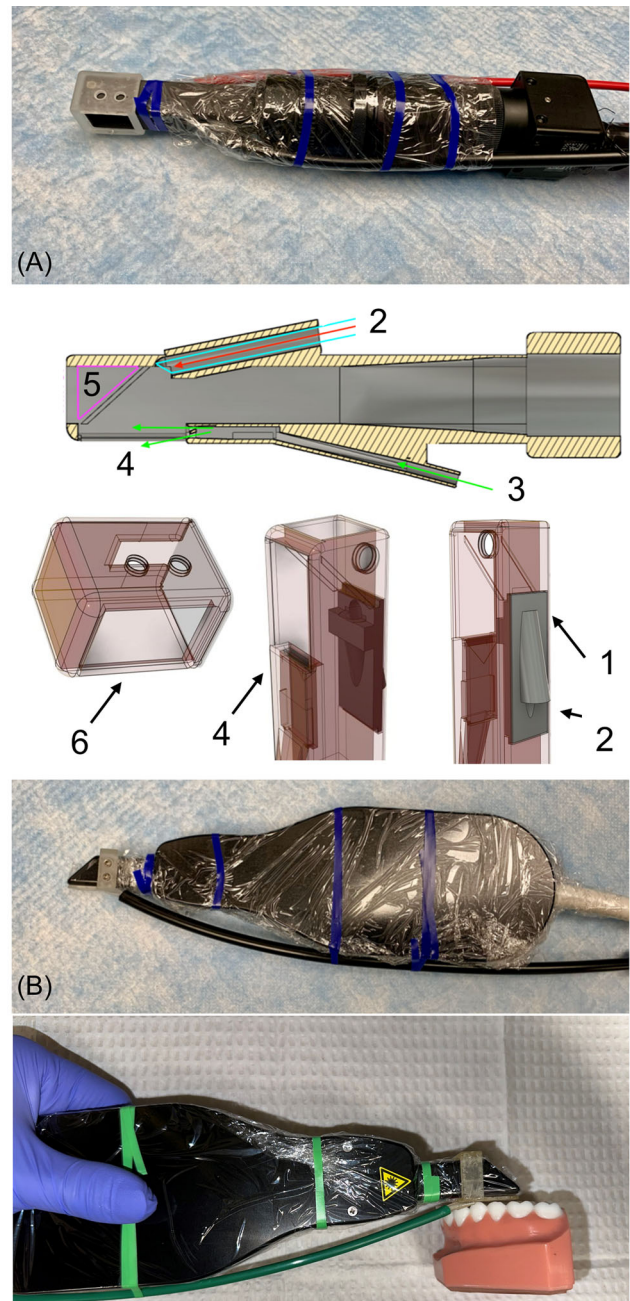


FIGURE 1 (A) Image of the fully assembled SWIR imaging handpiece that consists of three 3D printed autoclavable attachments, a 1 mm in diameter optical fiber for delivery of the SWIR light, an air nozzle, an assembly of two lenses, and an adjustable iris that is attached to the miniature InGaAs camera. Labeled diagrams of the probe body and two additional 3D printed components are also shown, where (1) is a 3D attachment that snaps into the probe body and holds the optical fiber and the Teflon plug that is inserted into the opening at (2), air enters the nozzle at (3), and exits at (4). The mirror attaches at (5) and another 3D printed component fits over the end of the probe body and makes contact with the tooth surface and functions as a bite block (6). Images of the CP-OCT handpiece are shown in (B) with an attached 3D printed autoclavable appliance with air nozzle. CP-OCT, cross polarization optical coherence tomography; SWIR, short wavelength infrared imaging.

appliance to prevent fogging of the imaging window. Images were imported into Dragonfly from ORS software for coregistration and analysis. A 3D Median filter was applied to reduce speckle noise in the images followed by 3D image registration to superimpose the lesion areas for all three visits. Images from the same sample at different visits also went through intensity normalization before quantitative measurement. The integrated reflectivity over the lesion depth (ΔR) which best represents the lesion severity was calculated by positioning a box within the lesion dimensions, calculating the mean pixel intensity in the box and multiplying by the lesion depth. Lesion depth (Ld) was measured on the registered lesion areas at the position of the maximum depth of the lesion. Lesion activity was evaluated as binary (arrested or active) based on detection of a TSL after image-processing. The TSL was measured along a ruler drawn at the center of the lesion orthogonal to the surface. All arrested lesions have TSLs measured as the distance between two adjacent intensity peaks (surface reflection from top of TSL to lesion underneath) measured after filtering. Statistical comparisons between suspected active and arrested lesion areas were performed in GraphPad Prism. RM-ANOVA with Tukey–Kramer multiple comparisons test was used to compare the CP-OCT data at 0, 3, & 6-months.

RESULTS

Out of the 30 test subjects recruited, 29 test subjects completed the study. Suspected lesions on 2 teeth were monitored on each test subject. Six of the remaining 58 lesions were determined to be sound since no lesions were visible in the CP-OCT images at any time points. A further 10 lesions were disqualified due to the inability to coregister the CP-OCT lesions at all three time-points yielding an CP-OCT sample size of 42 lesions. Visual monitoring indicated no changes in ICDAS scores for any of the lesions after 6-months.

Color and CP-OCT images extracted from 2 suspected active lesions, one that remained active and progressed further in depth and severity and a second lesion that became arrested are shown in Figure 2. The first lesion shows an increase in Ld and ΔR over 6 months with no TSL visible at the surface. CP-OCT images show a continual advance of the lesion in depth and area over time. In the second lesion example, a TSL is clearly visible at 3-months and after 6-months and the depth of the lesion has not appeared to increase significantly suggesting that it progressed from an active to arrested state (became arrested). The color images in Figure 2 show no changes in appearance between 0 and 6-months for either lesion.

Three parameters were calculated for each of the 42 lesions at each of the three time points from the CP-OCT

data. The lesion depth in microns (Ld), the lesion reflectivity integrated over the lesion depth (ΔR), and the thickness of the transparent surface zone (TSL) in microns. The mean \pm SD for each measurement are plotted in Figure 3. There were significant increases ($p < 0.05$) in the mean Ld and ΔR over the 6-month period for the 42 lesions. This suggests that most of the 42 lesions remained active and progressed in severity over the 6-month period. There were large increases in the mean TSL thickness for each 3-month period indicating that several of the lesions did indeed become arrested or remained arrested. At 6-months 14 of the 42 lesions manifested a distinct TSL indicating they were arrested. Six of the lesions had a TSL at month-0 and all 6 retained it over 6-months. The mean TSL thickness increased from 21 ± 25 (baseline month-0) to 115 ± 51 (month-6). Eight additional lesions formed new TSL's over 6-months and the TSL thickness increased significantly for the 6 arrested lesions from 49 ± 12 (month-0) to 150 ± 43 (month-6). Of the 14 lesions that had measurable TSLs at 6-months all 14 showed decreases in lesion severity (ΔR) from 0 to 6-months.

Analysis of the SWIR reflectance images at 0 and 6-months was more difficult than anticipated and only 48 of the 116 acquired videos were processed. Two parameters were calculated from the acquired time versus intensity curves, the change in intensity with drying (ΔI) and the initial delay before the rise in reflectivity (DEL). The 48 SWIR videos were separated into two groups defined as active and arrested based on the absence or presence of a TSL on the lesion. Due to the low number of lesions with TSLs, month-0 and 6 SWIR reflectance images were pooled together to yield 8 arrested videos and 40 active videos. There was a large and significant difference ($p < 0.05$) in the mean \pm SD for (DEL) 16 ± 8.9 versus 4.3 ± 5.1 s for active versus arrested lesions. For active lesions (ΔI) was higher, 18 ± 11 versus 13 ± 11 for active versus arrested lesions but the difference was not significant, ($p > 0.05$).

Figure 4A shows time-sequenced SWIR images of matched areas of the occlusal surface recorded during the 30 s of drying at 0 and 6-months. There is a very small lesion in the occlusal pit that was active at baseline and arrested at month-6 that can be seen in the CP-OCT images shown in Figure 4B along with color pictures of the area imaged in the SWIR. Profiles of the SWIR reflectance intensity are shown in Figure 4C extracted from the lesion area and a peripheral sound area during drying. The “active” lesion (month 0) shows a large delay of more than 20 s before a rapid rise in reflectivity as expected for an active lesion. The arrested lesion (month-0) manifests almost no delay before a more gradual rise in reflectivity as expected for an arrested lesion. However, since the rise in reflectivity occurs very late for the month-0 curve it is unclear whether all the changes in that curve were captured in the 30 s that were recorded.

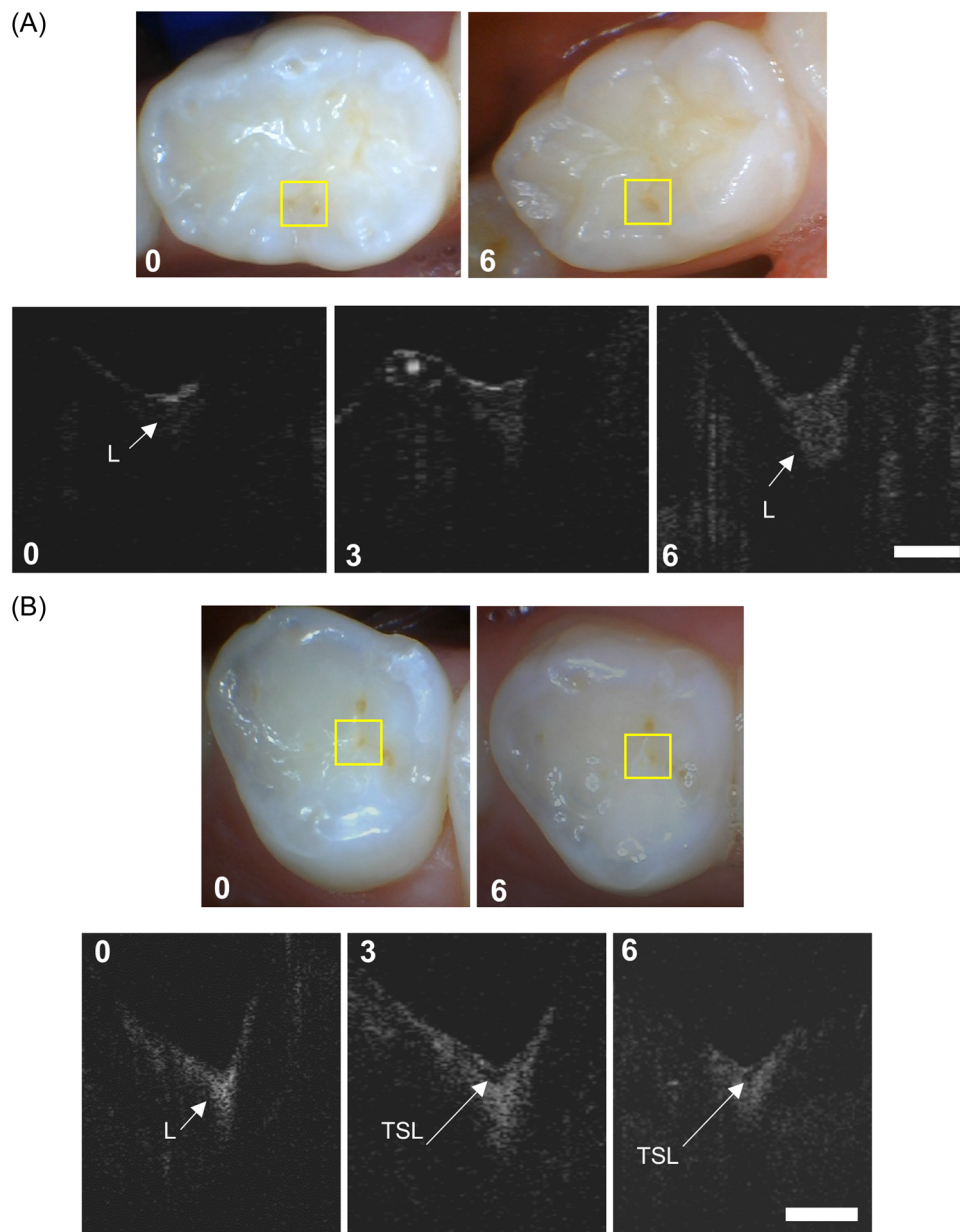


FIGURE 2 (A) Color and raw CP-OCT images of a suspected active lesion at 0, 3, and 6-months that remains active and progresses in severity. The position of the lesion in the color images is indicated by the yellow boxes. The lesion (L) is indicated in the CP-OCT b-scans at each time-point and the white bar represents a distance of 500 μm. No TSL was detected for this lesion. (B) Color and CP-OCT images of a suspected active lesion at 0, 3, and 6-months that appears to become arrested with the formation of a TSL at 3-months. CP-OCT, cross polarization optical coherence tomography; TSL, transparent surface layer.

DISCUSSION

This study was successful in recruiting a majority of test subjects with active lesions by choosing recently erupted primary teeth. Even though only a small number of those lesions that were initially active became arrested after 6 months with “lesion arrest” defined as the formation of a TSL measurable using CP-OCT, the number was sufficient to show a statistically significant increase ($p < 0.0001$) in the TSL thickness over time. Comparison of this study consisting of mainly “active” lesions in

which no TSL was present at baseline (36/42) with a previous study on permanent teeth where most lesions (62/63) had TSLs at baseline and there were no significant changes in lesion severity over 30-weeks¹² provides further confirmation that the TSL thickness is a key objective indicator of lesion activity. Furthermore, the TSL thickness provides a measure of the lesion activity that can be made at a single time-point. The mean TSL thickness for the 63 lesions at month-6 from the previous study was 184 ± 56 compared to 115 ± 51 for this study. The thickness was significantly higher

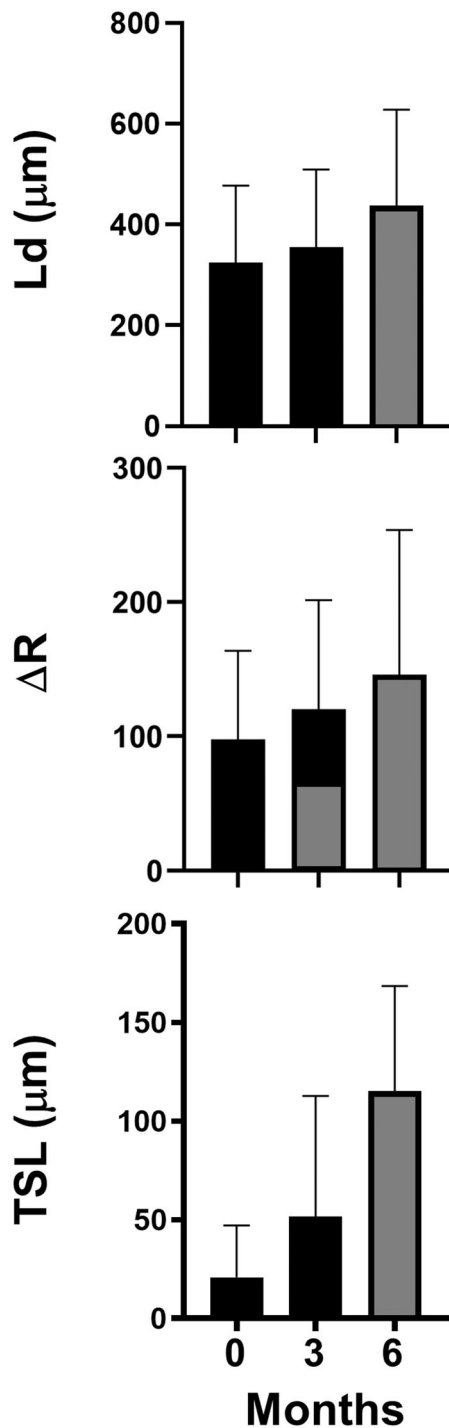


FIGURE 3 Plots of the measured mean \pm SD of the lesion depth (Ld) in microns, integrated reflectivity over the lesion depth (ΔR) in arbitrary units ($n = 42$) and the transparent surface zone thickness (TSL) in microns ($n = 14$) at 0, 3, and 6-months. Only the 14 lesions that had TSLs at 6-months are included for the TSL thickness. Bars containing the same color in each plot are statistically similar, RM-ANOVA with Tukey–Kramer multiple comparison test with ($p > 0.05$). TSL, transparent surface layer.

($p < 0.0001$, unpaired t -test) for the lesions on the permanent teeth in the previous study as would be expected for lesions that had a greater time to undergo remineralization. This is consistent with previous studies

of age-related differences in lesion structure based on histopathology.³

These two studies also show the poor reliability of visual/tactile indicators of lesion activity and severity such as color and texture. Active lesions were a recruitment criterion for both studies and out of the 111 primary and permanent teeth recruited for the two clinical studies only 37 were active according to CP-OCT imaging, 6 were sound and 69 were arrested and those 76 sites manifested no further change increase in severity over 6-months while the other suspected active lesions either progressed in severity ($n = 28$) or became arrested ($n = 7$). Moreover, visual monitoring with ICDAS indicated no changes in any of the lesions over 6-months for either study further confirming the low sensitivity of conventional visual monitoring.

In this study, there was a significant increase of the lesion depth (Ld) and the integrated reflectivity (ΔR) over the 6-month period suggesting that most of the lesions did not become arrested and actually progressed in severity. In vitro studies suggest that ΔR should decrease if all of the lesions become arrested and undergo major remineralization.^{8,9,33} As mineral is deposited into the lesion due to remineralization the overall reflectivity of the lesion decreases yielding a net decrease in ΔR . However, we observed TSL's in only 14 of the 42 lesions at 6-months indicating that only 1/3 of the lesions underwent enough remineralization to appear arrested. Therefore, the increases in ΔR and Ld are consistent with the majority of lesions remaining active during the duration of the study.

This was the first clinical study in which SWIR reflectance imaging was employed to assess lesion activity. Based on in vitro studies it was anticipated that (ΔI) the overall change in intensity would be significantly higher for active lesions versus arrested lesions.^{10,34,40,41} However, the time required for drying was much higher than encountered for in vitro studies and many of the active lesions did not sufficiently dry in 30 s.⁴¹ This influenced the ability to observe the full change in intensity for accurate calculation of (ΔI). For example, in Figure 4C the rise in intensity did not occur until after 20 s so it is unlikely that the ΔI calculated from that curve is reliable. The dehydration curves were also much noisier than expected making curve fitting difficult. These problems can be addressed in future studies by further increasing the air pressure and by further optimization of the air flow geometry in the probe to better penetrate the occlusal fits and fissures. The delay in the onset of the intensity change (DEL) appeared to be a better indicator of lesion activity than ΔI for this study. This onset delay (DEL) was ignored in early in vitro studies and was only recently discovered to be an indicator of lesion activity.^{10,34,40,41}

For active lesions there are exposed pores in the outer layer of the lesion, when those pores are filled with fluid they absorb the SWIR light lowering the reflectivity from the lesion. When the fluid is removed from the pores

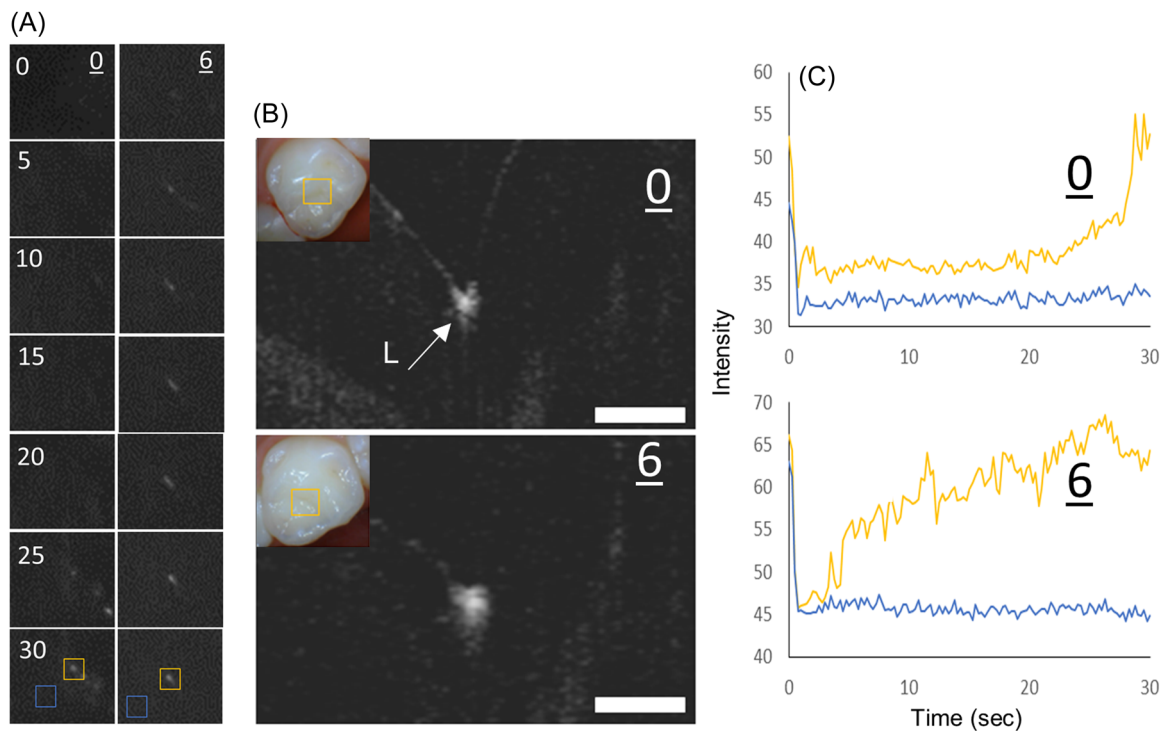


FIGURE 4 SWIR reflectance and CP-OCT images of another suspected active lesion that appears to become arrested at 6-months. (A) Time-sequence SWIR images of the lesion area from 0 to 30 s at 0 and 6-months are shown during drying. Lesion area is in yellow box and sound area is in the blue box. (B) CP-OCT scans at 0 and 6-months show a small pit and fissure lesion (L), the white bar represents 500 μm . Color images of the occlusal surface at 0 and 6-months are inset in each image and the lesion area monitored by SWIR is indicated by the yellow box. (C) The SWIR reflectance intensity is plotted between with time at 0 and 6-months at the lesion position shown by the small yellow boxes inset in the SWIR images at 30 s (yellow) and for adjacent sound areas (blue). CP-OCT, cross polarization optical coherence tomography; SWIR, short wavelength infrared imaging.

during drying the reflectivity rises. Arrested lesions have an outer highly mineralized TSL of low porosity with minimal fluid present between the lesion body and the surface so there is minimal delay before there is a rise in reflectivity during drying.⁴¹ It appears that this onset delay (DEL) is a good indicator of lesion activity that can be easily measured in vivo. It is desirable to be able to extract multiple indicators of lesion activity from the SWIR reflectivity versus time curves during drying as has been possible in in vitro studies where the curves were fit to extract additional information about the rate of increase in the reflectivity,⁴¹ not just DEL and ΔI as was done in this study and we plan on further development of the SWIR reflectance imaging handpiece for more rapid dehydration of the lesions.

Both OCT and SWIR imaging were done in contact with the tooth surface to minimize motion artifacts. Even so, several scans had to be repeated due to excessive movement during scanning for both OCT and SWIR reflectance imaging. In the case of SWIR imaging many of the image frames had to be corrected due to slight movement during the 30 s.

This study was not intended to be a clinical trial of fluoride varnish, therefore a non-fluoride varnish control

group was not used. Fluoride varnish was applied because it was the standard of care for patients of high caries risk and it was likely to increase the probability that more active lesions would undergo remineralization and become arrested.

CONCLUSION

This was the first clinical study to monitor changes in lesion structure and activity in primary teeth over time in vivo using CP-OCT and SWIR Imaging. The formation of a TSL at the surface of active lesions indicative of lesion arrest was observed using CP-OCT on multiple lesions. In addition, this was the first clinical study to use SWIR reflectance imaging to show differences in the dehydration dynamics between active and arrested lesions.

ACKNOWLEDGMENTS

The authors would like to acknowledge the support of NIDCR/NIH grant R01-DE027335 and the contributions of Cynthia Darling, Jacob Simon, Nai-Yuan Chang, and Donald Curtis.

CONFLICT OF INTEREST STATEMENT

The authors declare no conflict of interest.

ORCID

Daniel Fried  <https://orcid.org/0000-0002-5327-2558>

REFERENCES

1. Fejerskov O, Nyvad B, Kidd E, editors. *Dental Caries: the Disease and its Clinical Management*. Wiley Blackwell; 2015.
2. ten Cate JM, Arends J. Remineralization of artificial enamel lesions in vitro. *Caries Res*. 1977;11(5):277–86.
3. Kidd EA. The histopathology of enamel caries in young and old permanent teeth. *Br Dent J*. 1983;155(6):196–8.
4. Penning C, van Amerongen JP, Seef RE, ten Cate JM. Validity of probing for fissure caries diagnosis. *Caries Res*. 1992;26:445–449.
5. Angmar-Mansson B, al-Khateeb S, Tranaeus S. Caries diagnosis. *AADS Proc*. 1998;62(10):771–80.
6. Hume WR. Need for change in dental caries diagnosis. In: Stookey GK, editor. *Early Detection of Dental Caries, Annual Indiana Conference; Early Detection of Dental Caries*. Indiana University Press; 1996. p. 1–10.
7. Kidd EAM, Ricketts DNJ, Pitts NB. Occlusal caries diagnosis: a changing challenge for clinicians and epidemiologists. *J Dent*. 1993;21:323–31.
8. Jones RS, Fried D. Remineralization of enamel caries can decrease optical reflectivity. *J Dent Res*. 2006;85(9):804–8.
9. Kang H, Darling CL, Fried D. Nondestructive monitoring of the repair of enamel artificial lesions by an acidic remineralization model using polarization-sensitive optical coherence tomography. *Dent Mater*. 2012;28(5):488–94.
10. Lee RC, Darling CL, Fried D. Assessment of remineralization via measurement of dehydration rates with thermal and near-IR reflectance imaging. *J Dent*. 2015;43:1032–42.
11. Lee RC, Staninec M, Le O, Fried D. Infrared methods for assessment of the activity of natural enamel caries lesions. *IEEE J selected top quant*. *Electronics*. 2014;22(3):6803609.
12. Chan KH, Tom H, Lee RC, Kang H, Simon JC, Staninec M, et al. Clinical monitoring of smooth surface enamel lesions using CP-OCT during nonsurgical intervention. *Lasers Surg Med*. 2016;48(10):915–23.
13. Stookey GK. Quantitative light fluorescence: a technology for early monitoring of the caries process. *Dent Clin North Am*. 2005;49(4):753–70.
14. Ando M, Stookey GK, Zero DT. Ability of quantitative light-induced fluorescence (QLF) to assess the activity of white spot lesions during dehydration. *Am J Dent*. 2006;19(1):15–8.
15. Ando M, Ferreira-Zandoná AG, Eckert GJ, Zero DT, Stookey GK. Pilot clinical study to assess caries lesion activity using quantitative light-induced fluorescence during dehydration. *J Biomed Opt*. 2017;22(3):035005.
16. Kaneko K, Matsuyama K, Nakashima S. Quantification of early carious enamel lesions by using an infrared camera. In: Stookey GK, editor. *Annual Indiana Conference, Early detection of Dental Caries II*. Indiana University; 1999. p. 83–99.
17. Zakian CM, Taylor AM, Ellwood RP, Pretty IA. Occlusal caries detection by using thermal imaging. *J Dent*. 2010;38(10):788–95.
18. Usenik P, Bürmen M, Fidler A, Pernuš F, Likar B. Near-infrared hyperspectral imaging of water evaporation dynamics for early detection of incipient caries. *J Dent*. 2014;42(10):1242–7.
19. Lee C, Lee D, Darling CL, Fried D. Nondestructive assessment of the severity of occlusal caries lesions with near-infrared imaging at 1310 nm. *J Biomed Opt*. 2010;15(4):047011.
20. Lee RC, Darling CL, Fried D. Activity assessment of root caries lesions with thermal and near-infrared imaging methods. *J Biophotonics*. 2016;10(3):433–45.
21. Darling CL, Huynh GD, Fried D. Light scattering properties of natural and artificially demineralized dental enamel at 1310-nm. *J Biomed Opt*. 2006;11(3):034023.
22. Chung S, Fried D, Staninec M, Darling CL. Multispectral near-IR reflectance and transillumination imaging of teeth. *Biomed Opt Express*. 2011;2(10):2804–14.
23. Simon JC, Chan KH, Darling CL, Fried D. Multispectral near-IR reflectance imaging of simulated early occlusal lesions: variation of lesion contrast with lesion depth and severity. *Lasers Surg Med*. 2014;46(3):203–15.
24. Yang V, Zhu Y, Curtis D, Le O, Chang NYN, Fried WA, et al. Thermal imaging of root caries in vivo. *J Dent Res*. 2020;99(13):1502–8.
25. Colston BW, Everett MJ, Da Silva LB, Otis LL, Stroeve P, Nathel H. Imaging of hard and soft tissue structure in the oral cavity by optical coherence tomography. *Appl Opt*. 1998;37(19):3582–5.
26. Feldchtein FI, Gelikonov GV, Gelikonov VM, Iksanov RR, Kuranov RV, Sergeev AM, et al. In vivo OCT imaging of hard and soft tissue of the oral cavity. *Opt Express*. 1998;3(3):239–51.
27. Jones RS, Darling CL, Featherstone JDB, Fried D. Imaging artificial caries on the occlusal surfaces with polarization-sensitive optical coherence tomography. *Caries Res*. 2006;40(2):81–9.
28. Fried D, Xie J, Shafi S, Featherstone JDB, Breunig TM, Le C. Imaging caries lesions and lesion progression with polarization sensitive optical coherence tomography. *J Biomed Opt*. 2002;7(4):618–27.
29. Louie T, Lee C, Hsu D, Hirasuna K, Manesh S, Staninec M, et al. Clinical assessment of early tooth demineralization using polarization sensitive optical coherence tomography. *Lasers Surg Med*. 2010;42:898–905.
30. Nee A, Chan K, Kang H, Staninec M, Darling CL, Fried D. Longitudinal monitoring of demineralization peripheral to orthodontic brackets using cross polarization optical coherence tomography. *J Dent*. 2014;42(5):547–55.
31. Staninec M, Douglas SM, Darling CL, Chan K, Kang H, Lee RC, et al. Nondestructive clinical assessment of occlusal caries lesions using near-IR imaging methods. *Lasers Surg Med*. 2011;43(10):951–9.
32. Simon JC, Kang H, Staninec M, Jang AT, Chan KH, Darling CL, et al. Near-IR and CP-OCT imaging of suspected occlusal caries lesions. *Lasers Surg Med*. 2017;49(3):215–24.
33. Jones RS, Darling CL, Featherstone JDB, Fried D. Remineralization of in vitro dental caries assessed with polarization-sensitive optical coherence tomography. *J Biomed Opt*. 2006;11(1):014016.
34. Chang NN, Jew JM, Fried D. Lesion dehydration rate changes with the surface layer thickness during enamel remineralization. *Proc SPIE Int Soc Opt Eng*. 2018;10473:1–7.
35. Liu H, Chang NY, Gao W, Fried D. Infrared imaging confirms the role of the transparent surface zone in arresting dental caries. *Proc SPIE Int Soc Opt Eng*. 2021;11627:1–10.
36. Le MH, Darling CL, Fried D. Automated analysis of lesion depth and integrated reflectivity in PS-OCT scans of tooth demineralization. *Lasers Surg Med*. 2010;42(1):62–8.
37. Chan KH, Chan AC, Fried WA, Simon JC, Darling CL, Fried D. Use of 2D images of depth and integrated reflectivity to represent the severity of demineralization in cross-polarization optical coherence tomography. *J Biophotonics*. 2015;8(1-2):36–45.
38. Pitts N. “ICDAS”—an international system for caries detection and assessment being developed to facilitate caries epidemiology, research and appropriate clinical management. *Community Dent Health*. 2004;21(3):193–8.
39. Fried WA, Zhu Y, Yang V, Chang NY, Fried DA. SWIR imaging handpiece for the clinical assessment of lesion activity via

- dehydration. Preclinical assessment. *Proc SPIE Int Soc Opt Eng.* 2020;11217:1–7.
40. Lee RC, Kang H, Darling CL, Fried D. Automated assessment of the remineralization of artificial enamel lesions with polarization-sensitive optical coherence tomography. *Biomed Opt Express.* 2014;5(9):2950–62.
 41. Tressel J, Abdelaziz M, Fried D. Dynamic SWIR imaging near the 190 nm water absorption band for caries lesion diagnosis. *J Biomedical Opt.* 2021;26(5):056006.

How to cite this article: Zhu Y, Kim J, Lin B, Fried D. Monitoring lesion activity on primary teeth with CP-OCT and SWIR reflectance imaging. *Lasers Surg Med.* 2023;1–9.
<https://doi.org/10.1002/lsm.23677>